Structure, biosynthesis, and bioactivity of nostolysamides

Enleyona Weir,[1] Ivan Avertola,[1] and Wilfred A. van der Donk[1,*]

[1]Department of Chemistry and Howard Hughes Medical Institute, University of Illinois at Urbana-Champaign, Urbana, IL, 61822, USA

* corresponding author: vddonk@illinois.edu; 217 244 5360

Abstract

A recent genome mining study identified class II lanthipeptides encoded in *Nostoc punctiforme* PCC73102 that contain acyl groups conjugated to Lys side chains. The structure and bioactivity of these peptides, named nostolysamides, were not determined. In this study, we heterologously produced the nostolysamides by co-expression of the NpuA precursor peptide with an N-terminal SUMO tag with the class II lanthipeptide synthetase NpuM in *Escherichia coli.* We structurally characterized the NpuA-derived product and established the position of the thioether crosslinks. All four lanthionine and methyllanthionine residues were shown to have the DL configuration by Marfey's analysis. Tandem mass spectrometry as well as mutagenesis studies indicate an N-terminal non-overlapping methyllanthionine ring and three overlapping rings at the C-terminus for which the most likely ring pattern is proposed. After removal of the leader peptide, the resulting lanthipeptide exhibits antifungal activity against *Candida* species as well as antimicrobial activity against gram positive bacteria by disrupting cell membranes. The antibacterial activity is shown not to involve lipid II, consistent with the observed antifungal activity because fungi do not contain this bacterial cell wall precursor. The biosynthetic gene cluster also encodes an acetyltransferase NpuN that transfers long chain acyl groups to the side chain of a Lys residue in position 1 of the precursor peptide. In vitro studies of NpuN shows relatively broad substrate specificity with NpuN conjugating various acyl groups from acyl-CoA substrates to Lys1 in the nostolysamides. The acylation did not appreciably change the antifungal and antimicrobial activity of nostolysamide showing that it is not required for these activities.

Introduction

Invasive fungal infections have been estimated to affect over 6.5 million people worldwide each year, resulting in 3.8 million deaths.[1] This figure represents a significant increase over previous estimates, highlighting a growing global public health concern related to fungal infections and antimicrobial resistance. Candidiasis accounts for 24% of invasive fungal infections, making it a significant contributor.[1] *Candida albicans*, responsible for most *Candida* infections, is a commensal yeast that inhabits the skin and various mucosal surfaces of the human body.[2,3] *Candida* species are opportunistic pathogens, especially in immunocompromised patients, and can cause various diseases with high mortality rates.[1,4]

The rise of antifungal resistance poses a significant threat in the clinical setting. Therefore, efforts have been made to identify and characterize novel molecules with antifungal activity. Natural products constitute an important class of antifungal compounds. Amongst natural products, ribosomally synthesized and post-translationally modified peptides (RiPPs) are a rapidly growing family of molecules with a wide spectrum of biological activities, including antifungal activities.[5] Lanthipeptides are one of the largest families of RiPPs based on current genomes.[6] They are characterized by the presence of a thioether crosslink formed from a Ser/Thr and a Cys residue.[7] A previous study identified an antifungal two-component class I lanthipeptide system, pinensin A and B, which was isolated from *Chitinophaga*.[8] To date the pinensins constitute the only example of antifungal lanthipeptides, with most class II lanthipeptides displaying antimicrobial activity against Gram-positive bacteria. In this study, we characterize another lanthipeptide that exhibits activity against *Candida* species.

During the biosynthesis of class II lanthipeptides, a bifunctional enzyme (LanM) carries out dehydration of Ser and Thr residues to their corresponding dehydroamino acids dehydroalanine (Dha) and dehydrobutyrine (Dhb), and cyclization by Michael-type addition of Cys residues to the Dha/Dhb residues.[9] These post-translational modifications are performed on a precursor peptide (LanA) to form lanthionine (Lan from Ser/Cys) or methyllanthionine (MeLan from Thr/Cys) rings.[7] The modifications are typically introduced in the C-terminal part of the precursor peptide, LanA, called the core peptide, whereas an N-terminal leader peptide is removed by a peptidase to generate the mature natural product.[7] In some instances, additional modifications besides methyl(lanthionine) rings are introduced by enzymes encoded in the biosynthetic gene cluster (BGC).[10] For instance, general control non-repressible 5 (GCN5)-related N-acetyltransferases (GNATs) attach acyl groups.[11,12] In cases where acylation involves lipid chains, the lipidated peptides are more stable, often more potent, and typically membrane-active as a result of their hydrophobic tail.[13-15] Only a few known lanthipeptides are lipidated by GNATs, such as microvionin, the first example of a class III lanthipeptide that contains an N-terminal lipid.[16] Other N-terminally lipidated class III lanthipeptides are the goadvionins[17] and the lipoavitides.[18] Piel and Vagstad and colleagues discovered lanthipeptides in which not the N-terminus but the side chains of ornithines are lipidated.[19] They termed these RiPPs in which GNATs lipidate amino acid side chains selidamides, and characterized two members, kamptornamide and phaeornamide, encoded in cyanobacterial and marine α-proteobacterial BGCs, respectively.[19] The authors also showed that lanthipeptide BGCs encoding these GNATs are widespread, and for one BGC from *Nostoc punctiforme* PCC73102 (*npu*), they demonstrated acylation of the side chain of Lys in position 1.[19] The

structure and bioactivity of this lanthipeptide could not be determined because of the low production level. Independently, as part of a program to produce RiPPs using a Fast, Automated, Scalable, high-Throughput pipeline for RiPP discovery (FAST-RiPPs),[20] our group had targeted the same BGC. Here, we report further characterization of the product of the *npu* cluster and its bioactivity.

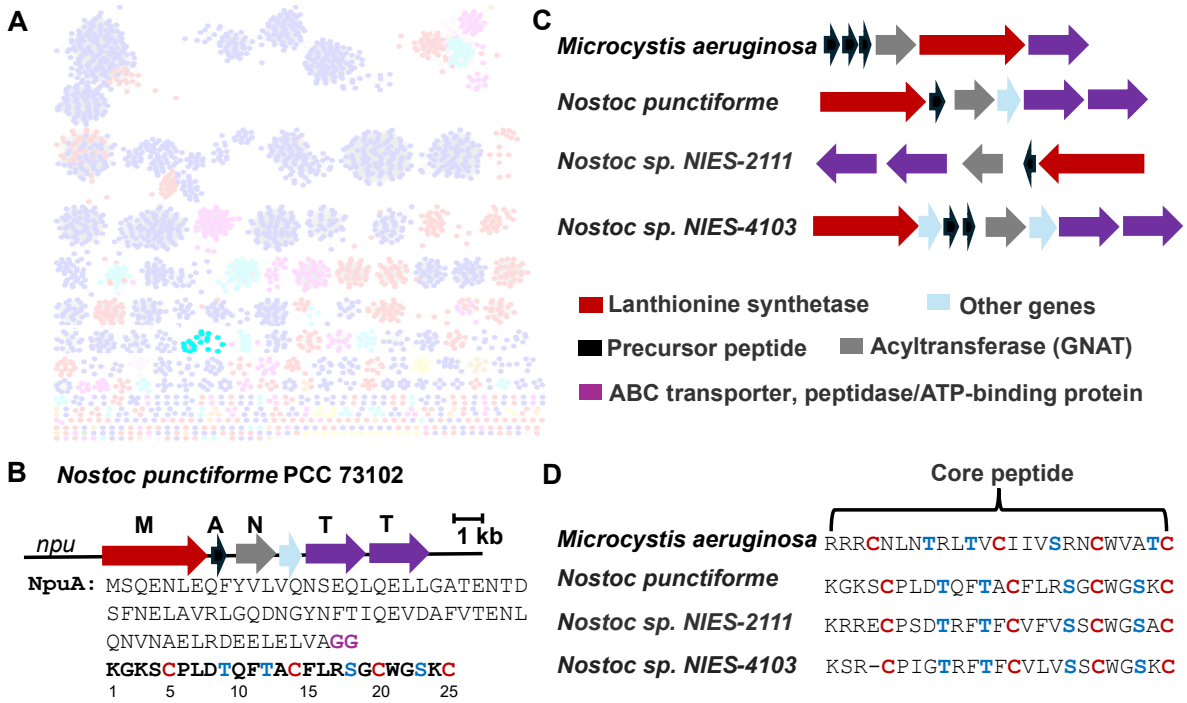

Figure 1. (**A**) Sequence similarity network (SSN) of predicted class II lanthipeptide precursor peptides generated with the Enzyme Function Initiative-Enzyme Similarity Tool with a permissive similarity cutoff (alignment score: 6; equivalent to an expectation value of 10^{-6}).[21] The SSN shown was visualized in Cytoscape v3.10.[22] Highlighted in cyan are the peptides that were previously designated cluster 65,[23] which is the topic of this study. (**B**) The nostolysamide BGC and the sequence of the precursor peptide NpuA. The predicted protease cleavage site for leader peptide removal is highlighted in purple and the core peptide is in bold. Residue numbering for the core peptide is indicated. (**C**) Representative BGCs associated with the 65 cluster in panel A, with genes colored according to predicted function. **(D**) Multiple

sequence alignment of selected core peptides of the 65 cluster, highlighting conserved residues.

Result and Discussion

Heterologous co-expression of the precursor peptide NpuA with NpuM

A previous bioinformatics genome-mining study mapped lanthipeptide diversity across sequenced genomes, identifying thousands of uncharacterized peptides with unique precursor peptide sequences that would yield new ring patterns.[23] Within the class II lanthipeptides reported in this bioinformatic study, a group of lanthipeptide precursors was identified in cyanobacteria that includes the *npu* BGC in *Nostoc punctiforme* PCC 73102 (**Fig. 1A**). As noted previously,[19] this BGC encodes a precursor peptide NpuA (WP_012412980.1), a class II lanthionine synthetase NpuM (WP_012412979.1), and a GNAT NpuN (WP_012412981.1) (**Fig. 1B**). To explore the distribution of *npu* BGCs, we also performed PSI-BLAST searches of the NCBI non-redundant database using the precursor peptide NpuA as query, yielding several BGCs that encode homologs of all three proteins (**Fig. 1C, D**). NpuA consists of a leader peptide (LP) of 78 amino acid residues, which is required for substrate recognition but does not undergo post-translational modification. This LP is a member of the Nif11 leader peptide family[24,25] and has a predicted Gly-Gly protease cleavage site, which is anticipated to be removed by the C39 peptidase domain of NpuT, a peptidase-containing ATP-binding cassette transporter (PCAT).[26,27] The core peptide of NpuA is composed of 25 amino acids, including two Thr residues, three Ser residues, and four Cys residues (**Fig. 1B**).

Co-expression of the bifunctional enzyme NpuM with N-terminally His_6-tagged NpuA in *Escherichia coli* and subsequent purification of NpuA using metal affinity

chromatography (IMAC) provided a fourfold dehydrated peptide. Subsequent *in vitro* removal of the leader peptide using LahT150,[26] the protease domain of a homolog of NpuT, provided peptide **1** and demonstrated that the four dehydrations (−72.04 Da) occurred in the core peptide (**Fig. 2A, Fig. S1, S2**). To assess whether **1** was fully cyclized, an N-ethylmaleimide (NEM) assay was conducted to detect any free cysteines in the modified product;[28] no NEM adducts were observed (**Fig. S3A**). Next, a dithiothreitol (DTT) assay was performed to test for the presence of dehydroamino acids in **1**. No adducts were observed (**Fig. S3A**). Collectively, these results indicate that **1** is fully cyclized.

Structural characterization of the modified peptides

As noted previously,[19] production levels of modified peptide from co-expression of NpuA with NpuM in *E. coli* were low. We were able to somewhat improve production by using a small ubiquitin-like modifier (SUMO) fusion at the NpuA N-terminus. The product of co-expression of His_6-SUMO-NpuA with NpuM again resulted in a fourfold dehydrated and fully cyclized product. While this improvement allowed structural characterization by tandem MS as discussed below, an initial screen of conditions for NMR demonstrated insufficient signal dispersion and solubility of peptide **1** (e.g. **Fig. S4**). The peptide was therefore subjected to liquid chromatography-tandem mass spectrometry (LC-MS) analysis to determine the ring pattern through collision-activated dissociation (CAD) fragmentation. The fragmentation data was analyzed using the Interactive Peptide Spectral Annotator (IPSA),[29] which generates predicted peptide fragments based on user-entered modifications. The tandem MS spectrum with IPSA annotations is presented in **Fig. 2B**. The fragmentation pattern is consistent with one MeLan ring formed from former Cys5 and Thr9. The very limited

fragmentation between Cys14 and Cys25 made it difficult to determine the pattern of the other three rings and suggested overlapping rings (**Fig. 2B**). In addition, the fragmentation pattern and IPSA annotation suggested that Ser4 was not dehydrated. To further confirm this conclusion, we replaced Ser4 with Ala by site-directed mutagenesis. Heterologous expression of the SUMO-NpuA-S4A mutant with NpuM yielded four dehydrations as observed for the wildtype (WT) peptide (**Fig. S5**), confirming that Ser4 is not dehydrated.

To provide further insights into the apparent overlapping ring pattern involving Cys14, Cys20, and Cys25, an additional site-directed mutagenesis experiment was performed on the *npuA* gene to replace Cys25 with Ala. Heterologous co-expression of the SUMO-NpuA-C25A mutant with NpuM resulted in four dehydrations (**Fig. 3A**). NEM and DTT assays were carried out after proteolysis with LahT150 to ensure that the mutant peptide was fully cyclized (**Fig. S2B**). The DTT assay of NpuM-modified NpuA-C25A (**2**) showed a 154 Da adduct, indicating the presence of one dehydroamino acid, as expected, since one ring could not form as a result of the mutation. Furthermore, no NEM adduct was observed suggesting that the remaining Cys residues were all cyclized (**Fig. S3B**). Compound **2** was subjected to tandem MS analysis (**Fig. 3B**). Most observed ions were also present in the tandem MS spectrum of **1**, but two diagnostic new ions were observed with **2**. The y_{12}^{+2} and y_{13}^{+2} ions are most consistent with a methyllanthionine ring between Dhb12 and Cys25 in the WT compound that has been disrupted in the NpuA-C25A mutant. These two fragment ions together with a new y_6 ion also suggest that Cys14 forms a ring with Ser18 and Cys20 with Ser23.

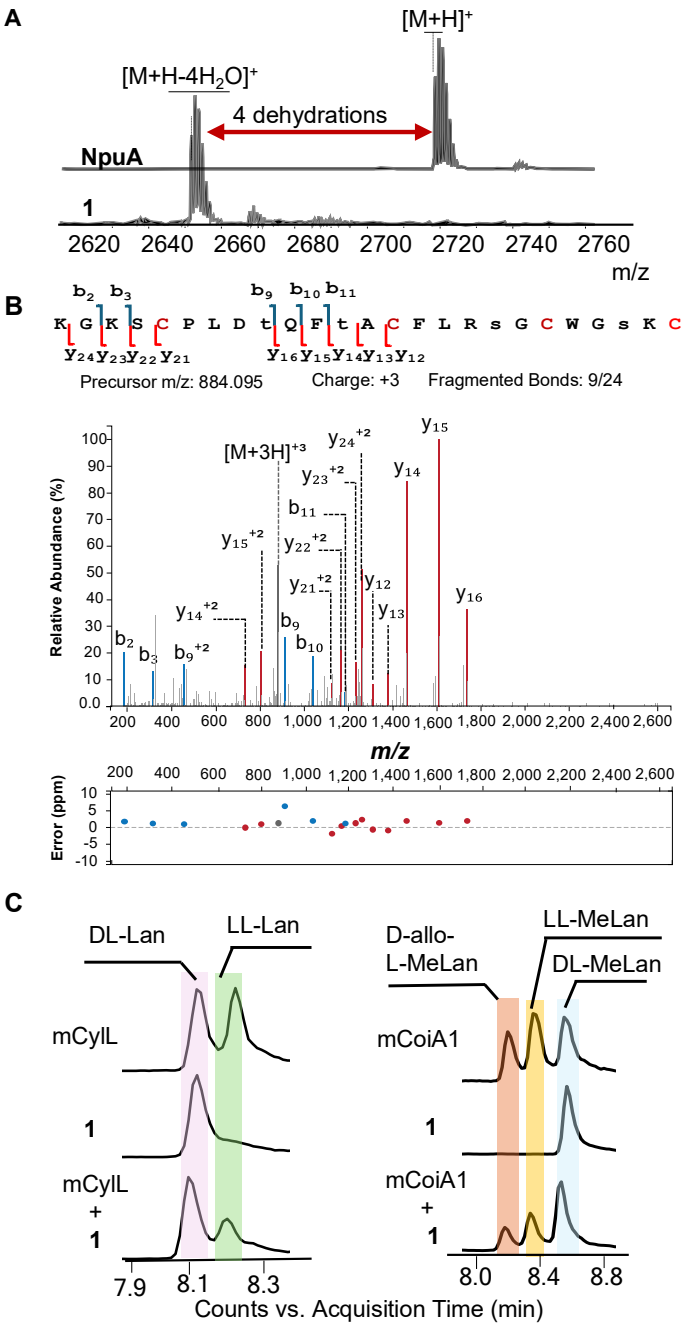

Figure 2. **Structural characterization of NpuM-modified SUMO-NpuA**. (**A**) MALDI-TOF mass spectra of NpuA before and after dehydration by NpuM, followed by cleavage with LahT150. NpuA, observed $[M+H]^+$ m/z 2719.3; calculated m/z=2723.3. NpuA co-expressed with NpuM and cleaved with LahT150: observed m/z $[M+H-4H_2O]^+$m/z=2651.2; calculated m/z=2651.2. (**B**) ESI-MS-MS data of **1** annotated with IPSA.[29] The input sequence involved dehydrated residues at the

positions indicated with lower-case letters. calculated m/z [M+3H-4H$_2$O]$^{3+}$ m/z=884.095, observed 884.095. (**C**) Marfey's analysis of the Lan and MeLan rings in **1**. mCylL and mCoiA1 were used as standards, as reported previously.[30]

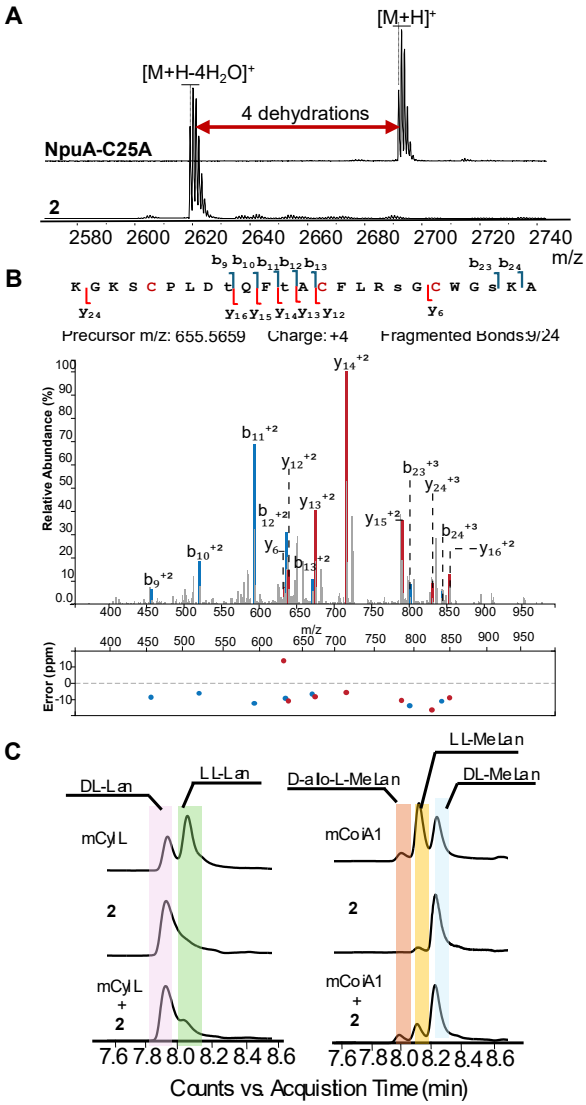

Figure 3. **Structural characterization of NpuM-modified SUMO-NpuA-C25A**. (**A**) MALDI-TOF mass spectra of NpuA-C25A before and after dehydration by NpuM, followed by cleavage with LahT150. NpuA-C25A, observed mass [M+H]$^+$ m/z=2691.7; calculated m/z=2691.3. Product **2**, observed mass [M+H-4H$_2$O]$^+$

m/z=2619.4; calculated m/z=2619.2. (**B**) ESI MS-MS data of product **2**. Plot generated by IPSA showing b and y ions when the input sequence (lower-case letters) involved dehydrated residues at the indicated positions.[29] Calculated m/z $[M+4H-4H_2O]^{4+}$ m/z=655.5659, observed 655.5712. (**C**) Marfey's analysis of the Lan and MeLan rings in compound **2**. mCylL and mCoiA1 were used as standards.[30]

Stereochemistry of Lan and MeLan

The stereochemistry of the Lan and MeLan residues in peptides **1** and **2** was analyzed using advanced Marfey's analysis. NpuM-modified SUMO-NpuA and SUMO-NpuA-C25A were subjected to hydrolysis under acidic conditions, followed by derivatization with the advanced Marfey reagent, Nα-(5-fluoro-2,4-dinitrophenyl)-L-leucinamide (L-FDLA).[30] Extracted ion chromatograms (EICs) using the masses for derivatized Lan ($[M-H]^-$ = 795.2373 Da) and MeLan $[M-H]^-$ = 809.2530 Da) were monitored by LC-MS and compared to standards of DL- and LL-Lan and DL-, LL-, and *allo*-LL-MeLan derivatized in the same manner. Separate injections as well as co-injections demonstrated that the configuration of the Lan and MeLan residues was DL (**Fig. 2C**).

The tandem MS data discussed above for the SUMO-NpuA-C25A mutant suggested a ring pattern for the WT product. Previous NMR studies have validated that the ring patterns of native lanthipeptides determined from tandem MS analysis of mutants are often correct.[23,31] However, some studies have shown that use of fragmentation patterns for mutants can be misleading with respect to the ring pattern of the native sequence in cases of competing non-enzymatic cyclization, or non-native enzymatic cyclization when the normally highly ordered cyclization process is

disrupted.[32-34] Therefore, complementary data that provide support that mutants are correctly cyclized are important. Non-enzymatic (methyl)lanthionine formation often results in loss of stereochemical control.[35] We therefore also determined the stereochemistry of the Lan and MeLan residues in NpuM-modified SUMO-NpuA-C25A (**2**). As shown in **Fig. 3C**, like peptide **1**, peptide **2** contains DL-Lan, and DL-MeLan, although a small amount of LL-MeLan was also observed. Together with the clean 4-fold dehydration, the stereochemical outcome suggests correct formation of the three (Me)Lan rings in mutant product **2**. Below, we will also show that this product has antifungal activity like product **1**, further supporting a native ring pattern.

Peptide 1 Exhibits Antimicrobial and Antifungal Activity

Peptide **1** was evaluated for antimicrobial activity against several Gram-positive, Gram-negative, and fungal strains using an agar diffusion assay. Compound **1** was dissolved in 5% aqueous dimethyl sulfoxide (DMSO) and spotted on agar plates. As a negative control, 5% aqueous DMSO was used, and kanamycin served as a positive control. Compound **1** demonstrated selective activity against several strains, as shown in **Fig. 4A**.

A

Strains	Activity/ MIC (µM)
Enterococcus faecium S235	-
Staphylococcus aureus NRS384	-
Klebsiella pneumoniae ATCC 27736	+/ <50
Acinetobacter baumanii ATCC 19606	-
Pseudomonas aeruginosa PAO1	-
Enterobacter cloacae ATCC 29893	-
Bacillus subtilis strain 168 (ATCC 23857)	+/ <3.75
Escherichia coli	+ 50
Candida tropicalis	+/ 6.25
Candida albicans	<100
Candida albicans SN250	+/ 6.25
Nakaseomyces glabratus (C. glabrata)	+/ 6.25
Candida krusei	<100
Aspergillus fumigatus	-
Lactococcus lactis	-
Micrococcus luteus	-

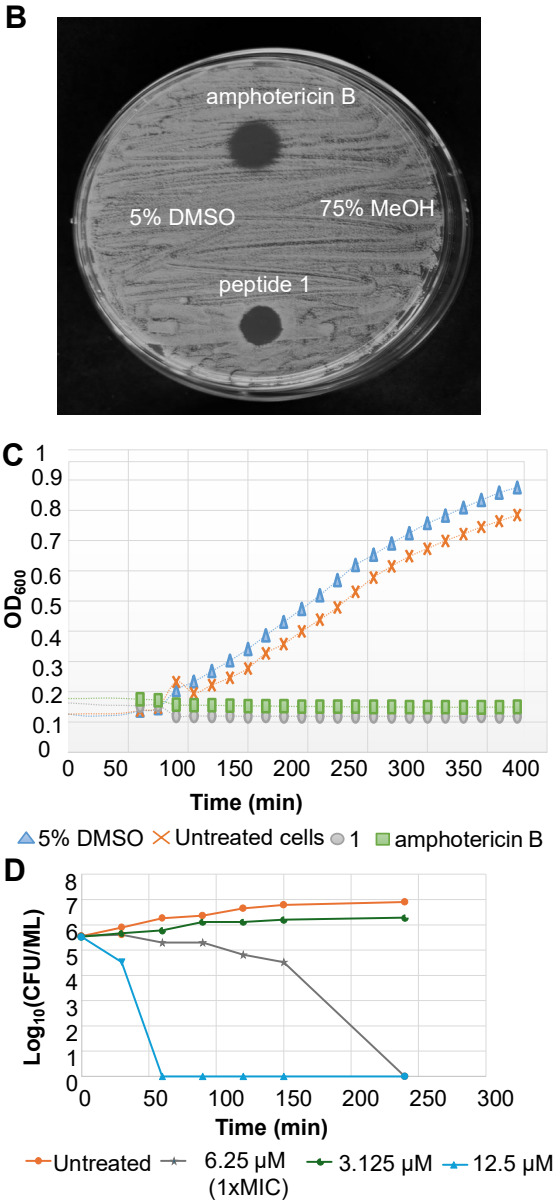

Figure 4. **Antimicrobial activity of nostolysamide (1)**. (**A**) Activity of peptide **1** against ESKAPE pathogens, fungal strains, Gram-negative, and Gram-positive bacteria; activity is indicated with + (growth inhibition) and – (no growth inhibition). The minimum inhibitory concentrations (MIC) were determined when antimicrobial activity was observed and are shown. (**B**) Agar diffusion assay with *Candida tropicalis* showing a clear zone of inhibition for peptide **1** (2 µL, 400 µM), the positive control, amphotericin B (2 µL, 1 mM), and no growth inhibition for the negative control 75% MeOH (2 µL) and 5% DMSO (2 µL). (**C**) Growth assay of *Candida tropicalis* displaying the optical

density at 600 nm (OD_{600}) for cells that were treated with peptide **1** (100 μM), amphotericin B (200 μM), and negative controls. (**D**) Time-kill assay starting with 1 x 10^5 colony-forming units (CFU) per mL of *Candida tropicalis* and monitoring the CFUs over 4 h using different concentrations of peptide **1**.

Peptide **1** inhibited the growth of *Bacillus subtilis* 168 (**Fig. S6**) and several *Candida* species (*Candida albicans* SN250*, Candida glabrata, Candida tropicalis*) at concentrations as low as 6.25 μM (**Fig. 4A, B; Fig. S7**). Using a broth dilution assay, weak activity was observed against some gram-negative bacteria, including *E. coli* and *Klebsiella pneumoniae* ATCC 27736 (Fig. S8).

As noted in the introduction and discussed below, Piel and coworkers denoted the products of the *npu* BGC as nostolysamides, with acylated side chains of a Lys residue in these compounds; two molecules containing different acyl groups were termed nostolysamides A and B.[19] Although peptide **1** does not feature an acyl group conjugated via an amide linkage to a Lys, we still consider it a congener of the products of the *npu* BGC and therefore will refer to it henceforth as nostolysamide C.

To assess the significance of the cyclic structure for activity, mutant **2** was also tested with both agar diffusion (**Fig. S9**) and broth dilution assays. Although the MIC value against *Candida tropicalis* increased more than a 10-fold, the dehydrated and cyclized mutant peptide was still active. Given the rarity of antifungal activity, we interpret these data as showing that the mutant peptide is still correctly cyclized but that the ring involving Cys25 is important for antifungal activity. Nostolysamide C is the first known class II lanthipeptide to exhibit activity against *Candida* species*,* a common cause of fungal infection in humans. To assess whether the compound is fungistatic or fungicidal, *Candida tropicalis* growth was monitored showing a decrease in colony forming units (CFUs) for both amphotericin B as positive control and nostolysamide C

compared to untreated cells (**Fig. 4D**). The data show that both molecules are fungicidal.

Class II lanthipeptides with antibacterial activity (lantibiotics) have diverse modes of action.[5] Nisin and mersacidin-like compounds bind to the cell wall precursor lipid II in bacteria.[36-41] Nostolysamide C was tested using a lipid II cycle-interfering assay that features a response regulator and sensor (LiaRS) assay. This system employs an engineered *Bacillus* strain in which a promoter controls the expression of the lacZ gene encoding the enzyme β-galactosidase in response to interference with the lipid II cycle.[42] When X-gal (a chromogenic substrate) was added to the medium, the positive control bacitracin produced the expected blue zone,[42] but nostolysamide C and the negative control ampicillin did not (**Fig. S10**). These findings suggest that nostolysamide C does not bind to lipid II, which is consistent with its observed antifungal effect since fungi do not contain lipid II.

Given the antibacterial and antifungal activity displayed by nostolysamide C, the most likely target is the cell membrane. We therefore investigated whether the nostolysamide C caused membrane depolarization by using a lipophilic cationic dye 3,3`-dipropylthiadixarbocyanine iodide (DiSC3(5)). In this assay, when the membrane of sensitive bacteria or fungi is depolarized, the fluorescence intensity of DiSC3(5) increases.[43,44] Addition of nostolysamide C indeed increased the fluorescence intensity like the positive control gramicidin[45,46] (**Fig. S11**), suggesting depolarization of the *Candida tropicalis* membrane.

Characterization of the GNAT-acetyltransferase product

Nostolysamide C is the product of NpuM modification of NpuA followed by leader peptide removal. The observed antifungal and antimicrobial activity was somewhat surprising because an additional gene, *npuN*, was previously shown to add long chain fatty acids to Lys1 of NpuA.[19] Hence, we had anticipated that the lipidation would be required for bioactivity. NpuN is a member of the GNAT-acyltransferase family.[47] Using NpuN as query, we generated an SSN of related GNATs (**Fig. S14**). The BGCs associated with cluster 1 of this SSN contain putative RiPP precursor peptides containing either an nitrile hydratase like leader peptide (NHLP) or a Nif11-related leader peptide, but they do not always encode a lanthionine synthetase (**Fig. S15**). A subset of these was shown in **Fig. 1B** and a more extensive list is provided in **Fig. S15**. Most of these BGCs also have an ABC transporter, suggesting that the acylated products are likely transported outside of the cells and have an extracellular function.

Heterologous co-expression of *npuA* and *npuN* in *E. coli* resulted in peptides containing adducts of 237.3 Da and 252.3 Da (**Fig. 5A**); these same adducts were also observed for the dehydrated and cyclized peptide upon coexpression of all three genes—*npuA*, *npuM*, and *npuN* (**Fig. 5B**). The two fatty acid adducts, corresponding to hexadecenoyl and hydroxyhexadecenoyl groups, were also observed by Piel and coworkers who termed them nostolysamide A and B.[19] Because of poor solubility, we were unable to purify the acylated products. We anticipated, based on previous data, that acylation occurred on Lys1.[19] To confirm the regioselectivity of acylation and test how strict this selectivity is, site-directed mutagenesis was used to replace Lys1 and Lys3 in the core peptide of NpuA with alanine. For completeness a double mutant NpuA-K1A/K3A was also constructed. When these mutant peptides were co-expressed with *npuN*, we observed an adduct only for NpuA-K3A (**Fig. S16**),

demonstrating that acylation occurs on Lys1 and that Lys3 and Lys24 cannot substitute when Lys1 is absent.

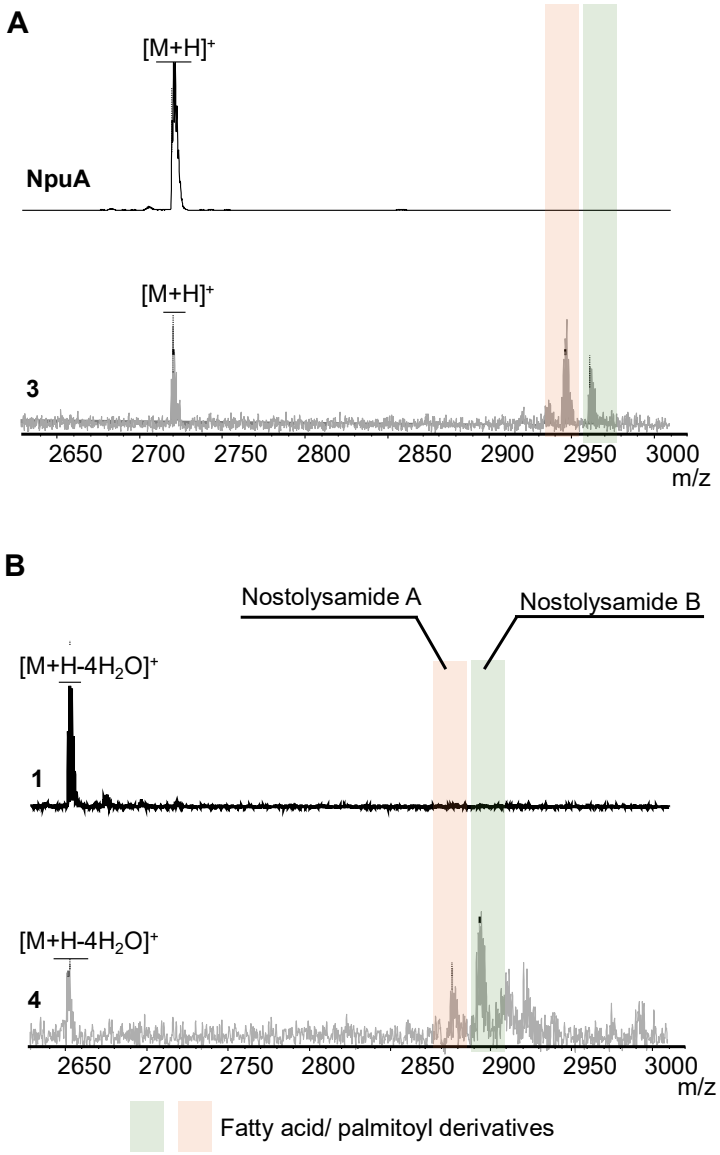

Figure 5. **MALDI-TOF MS analysis of NpuN-modified peptide products.** (**A**) MALDI-TOF mass spectra of NpuA and the peptide generated by coexpression of NpuA and NpuN, both treated with LahT150 in vitro**;** observed mass highlighted in orange and green, respectively: m/z 2957.2 and 2972.2. (**B**) MALDI-TOF mass spectra of the products of coexpression of NpuA and NpuM, and coexpression of

NpuA, NpuM, and NpuN showing lipidation of the products; observed mass highlighted in orange and green m/z 2887.8 and 2903.7.

NpuN displays substrate tolerance

The observed activity of NpuN was further evaluated *in vitro* by attaching a SUMO tag to its N-terminus to enhance solubility (**Fig. S17A**). His-SUMO-NpuN was expressed in *E. coli*, purified, and reacted with commercially available fatty acyl-CoAs and nostolysamide C (**1**) *in vitro* (**Fig. 6**). NpuN accepted acetyl-CoA, lauroyl-CoA, myristoyl-CoA, and oleoyl-CoA as substrates, resulting in the corresponding acylated nostolysamides (**Fig. 6A-E**). The peptide did not undergo complete modification and a mixture of acylated and non-acylated products was observed by MS that could not be purified because of the highly hydrophobic nature of the products, as also reported for the previously reported lipidated lanthipeptides kamptornamide and phaeornamide.[19] The reaction was enzyme catalyzed because no acylation was observed when NpuN was withheld from these assays. Although the poor solubility prevented kinetic characterization, palmitoyl-CoA resulted in the highest conversion, consistent with the C16 products observed during the co-expression experiments discussed above and reported previously.[19] Therefore, although it is possible that these acylated peptides may not represent the native products of *Nostoc punctiforme* PCC73102, the observation of C16 products by co-expression and the apparent in vitro preference for palmitoyl CoA suggests these are the physiological products. This hypothesis is also supported by the previous demonstration that the lipidated lanthipeptide phaeornamide produced in *E. coli* carried the same fatty acid as that detected in the native organism (*Pseudophaeobacter arcticus*).[19]

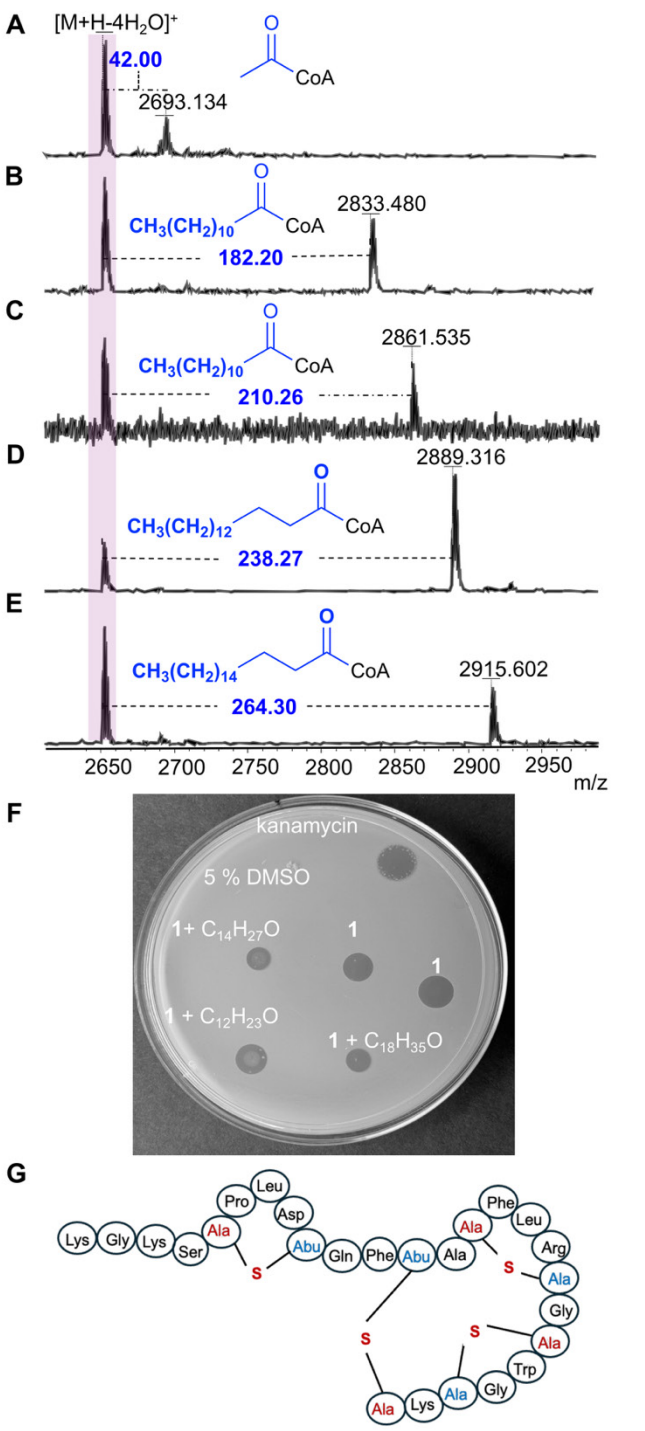

Figure 6. *In vitro* acylation of nostolysamide C by NpuN. (**A-E**) MALDI-TOF MS analysis of reactions containing acyl-CoA, His-SUMO-NpuN, and nostolysamide C. (**F**) Agar diffusion assay of palmitoylated, myristoylated, and laurylated nostolysamide against *B. subtilis* 168. (**G**) Structure of nostolysamide C.

GNAT enzymes involved in natural product acylation can serve self-resistance purposes or can enhance the biological activity of the compound.[48-50] The in vitro acylated nostolysamides mixtures were therefore used for agar diffusion assays against *B. subtilis* to determine whether the activity would be enhanced or abolished. For three different acyl groups, antibacterial activity was not significantly changed (**Fig. 6F**). The products were also subjected to the LiaRS assay, but no blue ring was observed (**Fig. S17B**). Hence, the function of the acylation of Lys1 is at present not clear.

Predicted structure of NpuN

An AlphaFold3 model[51] was generated for NpuN that revealed a tandem GNAT fold similar to other tandem GNAT proteins, a small group within the GNAT family (**Fig. S12A**).[52] Compared to the typical single-domain GNATs,[11,47,53] tandem GNAT proteins contain two GNAT-like domains within a single polypeptide. A DALI[54] search of the AlphaFold3 model of NpuN retrieved the single domain tabtoxin resistance protein (TTR) complexed with acetyl coenzyme A as the closest structural homolog (PDB ID 1GHE)[55] (**Fig. S12B**). Despite similar 3D folds, the sequence identity between NpuN and TTR is only 18.8%. (**Fig. S13A**). The acetyl-CoA binding site of GNATs is generated from a typical conserved P-loop motif [Q/R-X-X-G-X-G/A] that binds the diphosphate in acetyl-CoA.[47,56] Alignment of the sequence of TTR with NpuN identified the P-loop of NpuN in its N-terminal domain (**Fig. S13A**).

Virulence-induced protein F (VipF) from *Legionella hackeliae*, another tandem GNAT protein, contains P-loop sequences in both the N-terminal and a C-terminal domains.[57] Based on an alignment of VipF and NpuN, the conserved P-loop motif is clearly present in the N-terminal domain, but it is either absent or divergent in the C-

terminal region (**Fig. S13**). In several tandem GNAT proteins studied including VipF the N-terminal domain is mainly non-catalytic and plays structural or regulatory roles, while the C-terminal domain is catalytic.[52,57,58] However, exceptions occur for which the N-terminal domain is thought to be catalytic.[59] A structural alignment of VipF and the AlphaFold model of NpuN suggests the acylCoA binding site in the N-terminal GNAT domain is mostly buried in both proteins. In contrast, the C-terminal domain, which in NpuN lacks the clear consensus sequence for acetyl-CoA binding, has an open, solvent-accessible binding groove for both proteins (**Fig. S12B**). An AlphaFold3 model of the complex of NpuA with NpuN predicts that the peptide would bind preferentially to the C-terminal domain. In the model, potential catalytic residues Asp182 and His265 are positioned within about 5 Å of the Lys1 ε-amino group in the NpuA substrate (**Fig. S12C**). However, Asp and Tyr, which are suggested to serve as catalytic base to deprotonate substrate and catalytic acid to protonate the sulfur of the acylCoA in VipF,[57] are conserved in NpuN (**Fig. S12** and **S13**). Thus, experimental and/or structural data are needed to provide more insights into where catalysis takes place and which residues may be involved.

Discussion

As part of our genome mining efforts using the automated FAST-RiPPs platform,[20] a BGC from *Nostoc punctiforme* PCC73102 was refactored for expression in *E. coli*. Low production levels and difficulty with product isolation as well as the appearance of a literature report on the very same BGC[19] led us to not include our data in our previous report. However, the rapidly increasing interest in lipidated RiPPs and lipopeptides in general,[13,18,49,60-62] and the discovery that the product displays antifungal activity prompted attempts to improve production to facilitate structure

elucidation. Use of a fusion protein of the NpuA peptide and SUMO improved production sufficiently to carry out further biochemical characterization although yields remained low. Marfey's analysis demonstrated that all four (Me)Lan residues have the DL configuration, and tandem MS analysis on the product formed by NpuM from SUMO-NpuA-C25A suggests the ring pattern shown in **Fig. 6G**. Determination of ring pattern for lanthipeptides with overlapping rings using mutagenesis can be perilous, but the observed clean formation of a 4-fold dehydrated and cyclized product with NpuA-C25A, the observation of the same stereochemistry of the crosslinks, and the observation of retention of some of the antifungal activity collectively support the notion that the NpuA-C25A variant is converted to a ring pattern that is the same as WT with the exception of the ring involving Cys25. The ring pattern in **Fig. 6G** shows that the ring involving Cys25 is the largest macrocycle in the proposed structure. Previous studies have shown that large rings are usually formed last during lanthipeptide synthesis, when the smaller rings that are formed first bring two residues that are distant in the primary sequence closer together.[63,64] In turn, disruption of the cyclization process involving rings that are formed last typically does not affect the formation of the other rings, explaining why NpuA-C25A still formed a bioactive product. The decrease in antifungal activity of the resulting variant does indicate the importance of the ring between former Cys25 and Thr12 for bioactivity.

Only a few cyanobacterial natural products are known to have activity against fungal species.[65] Scytophycin is a broad-spectrum antifungal compound derived from *Scytonema*,[66] and nostocyclamide, derived from *Nostoc*, has a narrow spectrum activity that targets *Candida albicans*.[67] Another known cyanobacterial antifungal compound is calothrix A and B, isolated from *Calothrix,* which showed both antifungal and anticancer properties.[68] The preliminary mode of action studies suggest that

nostolysamide C targets the membrane and the greatly decreased activity of the C25A variant shows that cyclization is important for activity. Surprisingly, acylation of Lys1 did not increase antibacterial or antifungal activity, nor did it decrease such activity. Hence, NpuN is not likely to be a self-resistance enzyme, a role fulfilled by several other GNATs.[48] It is possible that increase in bioactivity is delicately dependent on the precise molecular nature of the acyl group or the organisms targeted. Tests of these hypotheses will require isolation of the nostolysamides from the producing organism and testing against organisms that co-inhabit the same environment as *Nostoc punctiforme* PCC73102, which was isolated from *Macrozamia* root. Given its complex life cycle involving vegetative cells, heterocysts, hormogonia and akinets,[69] the production and function of the nostolysamides will require further investigation.

General Experimental Procedures

Peptide and Protein Expression

Expression of His-NpuA, His-SUMO-NpuA, His-SUMO-NpuA/NpuM, His-SUMO-NpuA/NpuM/NpuN, His-SUMO-NpuA/NpuN, and His-LahT150, along with the NpuA variants, was performed using the same expression and purification method. For each sample, an overnight culture was grown from a single colony of freshly transformed *E. coli* BL21 (Tuner). This overnight culture was then diluted 1:100 into 1 L of LB broth and incubated at approximately 37 °C with shaking at 220 rpm until the culture reached an optical density of about 0.6. Co-expression with NpuN was adjusted so that cultures were grown at 30 °C until the desired OD_{600} was reached. The cultures were then placed on ice for about 30 min, followed by the addition of 0.5 mM isopropyl β-D-1-thiogalactopyranoside (IPTG). Afterward, the cultures were

incubated at 18 °C with shaking at 180 rpm overnight for 16-21 h. Subsequently, the cell pellets were harvested by centrifuging at 4500 x g for 15 min.

Generation of His-SUMO-NpuA variants

Site-directed mutagenesis was carried out using overlapping primers with the desired mutations (Table S2). The following sets of polymerase chain reaction (PCR) conditions were established using the modified Q5 Hot Start High-Fidelity DNA polymerase protocol. A reaction volume of 30 µL was prepared, containing 2× Q5 Hot Start Master Mix, 0.5 µM of each primer (both forward and reverse), 10-50 ng of DNA template, and DI H_2O, adjusted to a total volume of 50 µL. A temperature gradient was set for the annealing temperature. The initial denaturation was carried out for 40 s at 98 °C, followed by 26 cycles of denaturation (9 s, 95 °C), annealing (20 s, 56-72 °C), and elongation (4 min, 71.5 °C), with a final elongation step (72 °C) for 6 min. After amplification, 1 µL of Dpn1 enzyme was added to each 50 µL reaction, and the mixture was incubated at 37 °C for 45 min. Successful amplification was confirmed via gel electrophoresis. Next, 3 µL of amplified product was added to 50 µL of chemically competent NEB10Beta electrocompetent cells. The cells were electroporated using an electroporation instrument and recovered with 900 µL of NEB10Beta recovery media for 1 h, shaking at 37 °C. After recovery, cells were pelleted, and ~500 µL of supernatant was removed. The pellet was resuspended in the remaining media, and 50-100 µL was plated onto ampicillin plates. Plates were then incubated at 37 °C, after which single colonies were isolated and inoculated into 10 mL of LB containing ampicillin and grown overnight at 37 °C. Plasmid extraction was performed using Qiagen miniprep according to the manufacturer's protocol, and the plasmids were sent for sequencing at Plasmidsaurus to confirm successful mutagenesis.

Purification of peptides

Cell pellets were harvested and resuspended in Lysis buffer (20 mM Na_2HPO_4, 10 mM imidazole, 300 mM NaCl and 6 M guanidine hydrochloride, Gn-HCl, pH 7.5). This mixture was sonicated (40% amplitude, 4.4 s on, 5.5 off) for 6 min. The lysate mixture was centrifuged at 10,000 x g for 30 min. The supernatant was loaded onto an IMAC column equilibrated with Lysis buffer, using 0.5 mL of Ni resin per 1 gram of cell pellet. This step was followed by washing with 2–3 column volumes (CV) of Lysis buffer followed by Wash buffer 1 (20 mM Na_2HPO_4, 10 mM imidazole, 300 mM NaCl and 4 M Gn-HCl) The column was washed with 2-3 CV of Wash buffer 2 (20 mM Na_2HPO_4, 30 mM imidazole, 300 mM NaCl, pH 7.5) before eluting the peptide with 2-3 CV of Elution buffer (20 mM Na_2HPO_4, 1 M imidazole, 300 mM NaCl, pH 7.5).

Purification of Protease His-LahT150, His-NpuN, and His-SUMO-NpuN

Cell pellets were resuspended in protein Start buffer (20 mM Tris-HCl, 10 mM imidazole, 300 mM NaCl and 10% glycerol, pH 8.0) containing 4 mg/mL of lysozyme. This mixture was incubated at 4 °C, then lysed via sonication (40% amplitude, 4.4 s on, 5.5 off) for 6 min. The lysate mixture was centrifuged at 10,000 x g for 30 min. The supernatant was loaded onto an IMAC column equilibrated with protein Start buffer, using 0.5 mL of Ni resin per 1 gram of cell pellet. This step was followed by washing with 2–3 CV of protein Start buffer. The column was washed with 2-3 CV of protein Wash buffer (20 mM Tris-HCl, 30 mM imidazole, 300 mM NaCl and 10% glycerol, pH 8.0) before eluting the protein with 2-3 CV of protein Elution buffer (20 mM Tris-HCl, 300 mM imidazole, 300 mM NaCl and 10% glycerol, pH 8.0). Fractions were analyzed by SDS-PAGE using a 4–20% Tris gel at 150 V. The elution fraction was collected, concentrated, and buffer-exchanged into protein Storage buffer (20

mM Tris-HCl, 500 mM NaCl, and 10% glycerol, pH 8.0) using a 3 kDa MWCO Amicon filter. The fraction was then aliquoted and stored at −80 °C.

In vitro cleavage with LahT150

LahT150 cleavage reactions were performed at 25 °C for 18 h on the modified precursor peptides to obtain the modified core peptides for further purification and analysis. The elution buffer from peptide purification was exchanged to 50 mM Tris-HCl, 100 mM NaCl (pH 8.0) using an Amicon tube with a 3 kDa cutoff. LahT150 (2.5 mg/mL, approximately 136 μM) was added at 100 μL/L to the sample. The LahT150 assay was quenched by adding 0.1% v/v trifluoroacetic acid (TFA) in H_2O, and the mixture was centrifuged to remove precipitates. The supernatant was used for further purification.

HPLC purification of modified peptides

After Ni-NTA purification, the modified and unmodified LahT150-cleaved peptides were subjected to further purification on an Agilent 1260 II Infinity HPLC. The peptides were purified by RP-HPLC using a Hypersil GOLD C8 column (5 μm, 175 Å, 250 mm × 4.6 mm) with a linear gradient from 2% solvent B (100% MeCN with 0.1% TFA) in solvent A (0.1% TFA in water) to 100% solvent B over 33 min. The absorbance was monitored at 220 and 280 nm. Fractions containing the cleaved, modified core were identified by MALDI-TOF MS and lyophilized for further characterization.

NEM Assay

A literature procedure[28] was adapted. A 50 μL reaction was set up with 25-50 μM peptide dissolved in 50 mM Tris-HCl, pH 7.5 (25 μL), and 0.3 mM of fresh 1.0 mM

stock solution of TCEP (20 μL) that was incubated for 30 min at room temperature before 500 mM NEM (5 μL) was added. The reaction was incubated at room temperature for 3 h before using a C18 ziptip to prepare the sample for analysis by MALDI-TOF MS. For every free Cys in the peptide, a mass shift of +125 Da is expected.

DTT Assay

A literature procedure[28] was adapted. The peptide was dissolved in 50 μL of 100 mM Tris-HCl buffer, pH 7.5, to obtain a final concentration of 100 μM. *N*, *N*-diisopropylethylamine (DIPEA) and DTT were added to give final concentrations of 400 mM and 500 mM, respectively. The 50 μL reaction was incubated at room temperature for 3 h. After desalting with a C18 ziptip, the reaction was analyzed by MALDI-TOF MS.

High-Resolution Tandem Mass Spectrometry

The HPLC-purified peptides were injected onto a ThermoFisher Scientific Orbitrap Fusion electrospray ionization (HR-ESI) mass spectrometer using an Advion TriVersa Nanomate 100. The parameters used for MS(/MS) data acquisition included a resolution of 100,000 in positive mode, an isolation width of 0.5–2 m/z (MS/MS), and a normalized collision energy of 20, 25, and 30 (MS/MS). Data analysis was performed using the Xcalibur software.

Marfey's Analysis

For Marfey analysis, the two standards mCylL and mCoiA1, along with NpuA and mutants, were purified after heterologous expression in *E. coli* as described previously,[30] and derivatized with slight modifications. Dried peptides (~100 μg) were dissolved in 1 mL of 6 M DCl in D_2O for hydrolysis using a long glass vial. N_2 gas

was bubbled in the glass vials for 1 min. The reaction was heated to 120 °C and stirred for 20 h. Each reaction product was then dried using a rotary evaporator before being placed on a lyophilizer for 1 h to remove any remaining DCl. This step was followed by adding 0.6 mL of 0.8 M $NaHCO_3$ in H_2O and 0.4 mL of 4 mg/mL of Nα-(5-fluoro-2,4-dinitrophenyl)-l-leucinamide (L-FDLA) in acetonitrile. Next, the glass vials were stirred in the dark at 67 °C for 3 h. Subsequently, 100 μL of 6 M HCl was added to the derivatization product, and the mixture was vortexed. The mixture was placed on a lyophilizer to dry, and the residue was resuspended in 500 μL of acetonitrile. The resuspension mixture was centrifuged at high speed for 10 min, and the supernatant was collected and analyzed on an Agilent 6545 LC/Q-TOF instrument using a Kinetex 1.7 μm F5 100 Å, LC column (100 × 2.1 mm; Phenomenex; part no.: 00D-4722-AN) at a constant flow rate of 0.4 mL/min. The eluting system consisted of a gradient of 5-80 % of Solvent B (MeCN with 0.1% formic acid) in Solvent A (water with 0.1% formic acid). Chromatographic separation was obtained for each derivatized diastereomer and the identity of the NpuA samples was confirmed by co-injection and extracting the exact mass for derivatized MeLan (m/z 809.25299) and Lan (m/z 795.23734).

Agar Well Diffusion Assays to Determine Antimicrobial Activity

Agar well diffusion growth-inhibition assays were conducted using the peptide following a biosynthesis protocol from our previous report.[20] Peptides were dissolved in 5% DMSO to achieve a starting concentration of 0.5 mg/mL. Agar plates were prepared by making 1% agar with the desired media, approximately 20 mL for the bottom agar. The top agar was prepared by adding 200 μL of the overnight cell culture to 20 mL of melted agar cooled to about 55 °C. The cultured agar was then poured onto the bottom agar to solidify. The dissolved peptide was directly spotted

onto the solidified plate. For the fungi agar assay, sterile cotton swabs or Q-tips were used to streak the overnight fungi culture on the plate before spotting the dissolved peptide. The dried plates were incubated at 37 °C for 18 h, and the presence or absence of zones of growth inhibition determined the activity. The negative control was 5% DMSO, and the positive control was kanamycin for the bacterial assay or amphotericin B for the fungal assay.

Minimal Inhibitory Concentration (MIC) Determination

The method was modified from a previously described procedure.[70] The MIC was determined using the standard doubling dilution method with Lysogeny broth (LB), Mueller-Hinton broth (MHB), or RPMI 1640 for fungal species. All tests with the examined wells were performed with three biological replicates. Overnight cultures were inoculated and grown for an additional 4 h before adjusting the bacterial culture to approximately 10^5 CFU per mL. The assay was set up with wells containing various concentrations, ranging from 0.78 μM to 200 μM of the tested peptide. A positive control was included with kanamycin or amphotericin B, a negative control with just 5% DMSO, and a row with only medium. For the antifungal MIC against *Candida* species, as previously described,[70] an inoculum of 1×10^5 cells in 190 μL of RPMI 1640 medium was added to 96-well polystyrene microplates with different concentrations of the tested peptide and amphotericin B. After incubation at 37 °C for 18 h, the OD_{600} was measured using a plate reader. The MIC was defined as the lowest concentration at which the tested peptide caused growth inhibition.

LiaRS assay

The method followed the previously described protocol with modifications.[42] An overnight culture of *B. subtilis* BSF2470 was grown to an OD_{600} of 1.0 before dilution with 0.7% molten LB agar containing 20 mg/mL X-Gal/DMF. The molten agar was

overlayed on a solidified bottom agar. The plates were allowed to cool and dry on the bench at room temperature for 30 min. Then samples were spotted directly on the plates in the following manner: 100 mg/mL ampicillin (2 μL - negative control), 35 mM bacitracin (2 μL - positive control), 2 μL of 5% DMSO, and 2 μL of 200 μM peptide **1**. Plates were left for 45 min before being placed in a 37 °C incubator for 18 h. A blue ring around the zone of inhibition indicates the compound targets the bacterial cell wall or membrane, including through lipid II associated processes.

Time killing assay of peptide 1 against *Candida tropicalis*

Time-killing assays were performed according to a previously described protocol, with modifications.[71] Briefly, a growth curve was generated in the absence of the tested peptide to determine the doubling time of *Candida tropicalis*. The experiment was conducted in triplicate. An overnight culture was inoculated and diluted 100-fold in RPMI medium. The cells were incubated at 37 °C, then grown for an additional 4 h before being incubated at 37 °C to an OD_{600} of 1.0. The cell concentration was adjusted to 5×10^5 CFU/mL. Fungi were then incubated at half the MIC and the MIC of peptide **1**. Cells treated with 5% DMSO were used as a control. At the 4-hour time point, 10 μL was taken from each sample, diluted 1000-fold in RPMI, and plated on Sabouraud Dextrose agar plates. After overnight incubation at 37 °C, colonies on the plates were counted and expressed as colony-forming units per mL to generate the plot.

DiSC3(5) Assay[43]

Cells were grown in potato dextrose (PD) medium until logarithmic growth was obtained. Cells were diluted to an OD600 of 0.2 in pre-warmed PD supplemented with 0.5 mg/mL BSA. Fluorescence measurements were performed using a Tecan Plate Reader Infinite F200 with an excitation wavelength of 622 nm and emission at

670 nm. Membrane depolarization was indicated by an increase in fluorescence intensity due to dye release into the extracellular medium. Cells (135 μL) were transferred to the microtiter plate and the fluorescence was recorded for 2–3 min in order to obtain values for medium and cell background. After obtaining a baseline, DiSC3(5) dissolved in DMSO (100 μM) was added to each well to a final concentration 1 μM DiSC3(5) and 1% DMSO. Maintaining 1% DMSO was critical for good solubility and fluorescence of the dye. Fluorescence was measured until a stable signal intensity was achieved, followed by addition of the compound of interest. To separate wells for the positive control 1 μM of channel-forming peptide gramicidin S was used. Nostolysamide C was used for the tested compound, 10 μL of the 50 μM and 100 μM were added to separate wells. 5 % DMSO was used as a negative control. Fluorescence readings were recorded over 60 min.

***In vitro* reaction with His-SUMO-NpuN**

The NpuA peptide was dissolved in 5% DMSO to a concentration of 50 μM. His-SUMO-NpuN was added to a final concentration of 17 μM, along with 200 μM of fatty acyl-CoA. Tris-HCl at pH 8.5 was added to make the total reaction volume 100 μL. The reaction was incubated at 37 °C and analyzed by MALDI-TOF MS after 16-18 h.

ASSOCIATED CONTENT

Supporting Information

Figures S1-S17 showing mass spectrometry and bioactivity data, and AlphaFold models, and Tables S1-S5 with gene sequences and accession numbers, primers, and plasmids used (PDF).

AUTHOR INFORMATION

Acknowledgements

The authors thank Youran Luo for help with Marfey's analysis, Dr. Chengyou Shi for the construction of the original plasmid encoding NpuA and NpuM, and Dr. Chandrashekhar Padhi for helpful discussions regarding fungal assays.

Funding

This work was supported in part by the National Institutes of Health (Grant R01 AI144967 to W.A.V.). W.A.V. is an Investigator of the Howard Hughes Medical Institute.

Notes

The authors declare no competing financial interests.

Data availability

Raw data are deposited on Mendeley and will be released upon publication. Weir, E.; van der Donk, W.A. (2026), Data associated with "Structure and biosynthesis of nostolysamides", Mendeley Data, V1, doi: 10.17632/bczwrs7nr9.1.

References

(1) Denning, D. W. Global incidence and mortality of severe fungal disease. *Lancet Infect. Dis.* **2024**, *24*, e428-e38.
(2) Chang, C.-K.; Kao, M.-C.; Lan, C.-Y. Antimicrobial activity of the peptide LfcinB15 against Candida albicans. *J. Fungi* **2021**, *7*, 519.
(3) Sardi, J. C. O.; Scorzoni, L.; Bernardi, T.; Fusco-Almeida, A. M.; Mendes Giannini, M. J. S. Candida species: current epidemiology, pathogenicity, biofilm formation, natural antifungal products and new therapeutic options. *J. Med. Microbiol.* **2013**, *62*, 10-24.
(4) Ben-Ami, R. Treatment of invasive candidiasis: a narrative review. *J. Fungi* **2018**, *4*, 97.
(5) Ongpipattanakul, C.; Desormeaux, E. K.; DiCaprio, A.; van der Donk, W. A.; Mitchell, D. A.; Nair, S. K. Mechanism of action of ribosomally synthesized and post-translationally modified peptides. *Chem. Rev.* **2022**, *122*, 14722-814.
(6) Li, H.; Ding, W.; Zhang, Q. Discovery and engineering of ribosomally synthesized and post-translationally modified peptide (RiPP) natural products. *RSC Chem. Biol.* **2024**, *5*, 90-108.
(7) Repka, L. M.; Chekan, J. R.; Nair, S. K.; van der Donk, W. A. Mechanistic understanding of lanthipeptide biosynthetic enzymes. *Chem. Rev.* **2017**, *117*, 5457-520.
(8) Mohr, K. I.; Volz, C.; Jansen, R.; Wray, V.; Hoffmann, J.; Bernecker, S.; Wink, J.; Gerth, K.; Stadler, M.; Müller, R. Pinensins: the first antifungal lantibiotics. *Angew. Chem. Int. Ed.* **2015**, *54*, 11254-8.
(9) Xie, L.; van der Donk, W. A. Post-translational modifications during lantibiotic biosynthesis. *Curr. Opin. Chem. Biol.* **2004**, *8*, 498-507.
(10) Funk, M. A.; van der Donk, W. A. Ribosomal natural products, tailored to fit. *Acc. Chem. Res.* **2017**, *50*, 1577-86.
(11) Shirmast, P.; Ghafoori, S. M.; Irwin, R. M.; Abendroth, J.; Mayclin, S. J.; Lorimer, D. D.; Edwards, T. E.; Forwood, J. K. Structural characterization of a GNAT family acetyltransferase from Elizabethkingia anophelis bound to acetyl-CoA reveals a new dimeric interface. *Sci. Rep.* **2021**, *11*, 1274.
(12) Favrot, L.; Blanchard, J. S.; Vergnolle, O. Bacterial GCN5-related N-acetyltransferases: from resistance to regulation. *Biochemistry* **2016**, *55*, 989-1002.
(13) Guo, L.; Wang, C.; Broos, J.; Kuipers, O. P. Lipidated variants of the antimicrobial peptide nisin produced via incorporation of methionine analogs for click chemistry show improved bioactivity. *J. Biol. Chem.* **2023**, *299*, 104845.
(14) Hamley, I. W. Lipopeptides: from self-assembly to bioactivity. *Chem. Commun.* **2015**, *51*, 8574-83.
(15) Esposito, S.; Krick, A.; Pasquier, O.; Bonche, F.; Ingenito, R.; Magotti, P.; Bianchi, E.; Monteagudo, E.; Gallo, M.; Cicero, D. O.; Orsatti, L.; Veneziano, M.; Caretti, F.; Mele, R.; Roversi, D.; Gennari, N.; Brasseur, D.; Gauzy-Lazo, L.; Duclos, O.; Mauriac, C.; Illiano, S.; Mallart, S. Fatty acid acylated peptide therapeutics: discovery of omega-n oxidation of the lipid chain as a novel metabolic pathway in preclinical species. *J. Pharm. Biomed. Anal.* **2023**, *227*, 115256.
(16) Wiebach, V.; Mainz, A.; Siegert, M. J.; Jungmann, N. A.; Lesquame, G.; Tirat, S.; Dreux-Zigha, A.; Aszodi, J.; Le Beller, D.; Süssmuth, R. D. The anti-staphylococcal lipolanthines are ribosomally synthesized lipopeptides. *Nat. Chem. Biol.* **2018**, *14*, 652-4.

(17) Kozakai, R.; Ono, T.; Hoshino, S.; Takahashi, H.; Katsuyama, Y.; Sugai, Y.; Ozaki, T.; Teramoto, K.; Teramoto, K.; Tanaka, K.; Abe, I.; Asamizu, S.; Onaka, H. Acyltransferase that catalyses the condensation of polyketide and peptide moieties of goadvionin hybrid lipopeptides. *Nat. Chem.* **2020**, *12*, 869-77.
(18) Ren, H.; Huang, C.; Pan, Y.; Dommaraju, S. R.; Cui, H.; Li, M.; Gadgil, M. G.; Mitchell, D. A.; Zhao, H. Non-modular fatty acid synthases yield distinct N-terminal acylation in ribosomal peptides. *Nat. Chem.* **2024**, *16*, 1320-9.
(19) Hubrich, F.; Bösch, N. M.; Chepkirui, C.; Morinaka, B. I.; Rust, M.; Gugger, M.; Robinson, S. L.; Vagstad, A. L.; Piel, J. Ribosomally derived lipopeptides containing distinct fatty acyl moieties. *Proc. Natl. Acad. Sci. U S A* **2022**, *119*, e2113120119.
(20) Ayikpoe, R. S.; Shi, C.; Battiste, A. J.; Eslami, S. M.; Ramesh, S.; Simon, M. A.; Bothwell, I. R.; Lee, H.; Rice, A. J.; Ren, H.; Tian, Q.; Harris, L. A.; Sarksian, R.; Zhu, L.; Frerk, A. M.; Precord, T. W.; van der Donk, W. A.; Mitchell, D. A.; Zhao, H. A scalable platform to discover antimicrobials of ribosomal origin. *Nat. Commun.* **2022**, *13*, 6135.
(21) Oberg, N.; Zallot, R.; Gerlt, J. A. EFI-EST, EFI-GNT, and EFI-CGFP: Enzyme Function Initiative (EFI) web resource for genomic enzymology tools. *J. Mol. Biol.* **2023**, *435*, 168018.
(22) Shannon, P.; Markiel, A.; Ozier, O.; Baliga, N. S.; Wang, J. T.; Ramage, D.; Amin, N.; Schwikowski, B.; Ideker, T. Cytoscape: a software environment for integrated models of biomolecular interaction networks. *Genome Res.* **2003**, *13*, 2498-504.
(23) Walker, M. C.; Eslami, S. M.; Hetrick, K. J.; Ackenhusen, S. E.; Mitchell, D. A.; van der Donk, W. A. Precursor peptide-targeted mining of more than one hundred thousand genomes expands the lanthipeptide natural product family. *BMC Genom.* **2020**, *21*, 387.
(24) Li, B.; Sher, D.; Kelly, L.; Shi, Y.; Huang, K.; Knerr, P. J.; Joewono, I.; Rusch, D.; Chisholm, S. W.; van der Donk, W. A. Catalytic promiscuity in the biosynthesis of cyclic peptide secondary metabolites in planktonic marine cyanobacteria. *Proc. Natl. Acad. Sci. U.S.A.* **2010**, *107*, 10430-5.
(25) Haft, D. H.; Basu, M. K.; Mitchell, D. A. Expansion of ribosomally produced natural products: a nitrile hydratase- and Nif11-related precursor family. *BMC Biol.* **2010**, *8*, 70.
(26) Bobeica, S. C.; Dong, S. H.; Huo, L.; Mazo, N.; McLaughlin, M. I.; Jimenéz-Osés, G.; Nair, S. K.; van der Donk, W. A. Insights into AMS/PCAT transporters from biochemical and structural characterization of a double glycine motif protease. *eLife* **2019**, *8*, e42305.
(27) Lin, D. Y.; Huang, S.; Chen, J. Crystal structures of a polypeptide processing and secretion transporter. *Nature* **2015**, *523*, 425–30.
(28) Ayikpoe, R. S.; van der Donk, W. A. Peptide backbone modifications in lanthipeptides. *Methods Enzymol.* **2021**, *656*, 573-621.
(29) Brademan, D. R.; Riley, N. M.; Kwiecien, N. W.; Coon, J. J. Interactive peptide spectral annotator: A versatile web-based tool for proteomic applications. *Mol. Cell. Proteom.* **2019**, *18*, S193-S201.
(30) Luo, Y.; Xu, S.; Frerk, A. M.; van der Donk, W. A. Facile method for determining lanthipeptide stereochemistry. *Anal. Chem.* **2024**, *96*, 1767-73.
(31) Tang, W.; van der Donk, W. A. Structural characterization of four prochlorosins: a novel class of lantipeptides produced by planktonic marine cyanobacteria. *Biochemistry* **2012**, *51*, 4271-9.

(32) Thibodeaux, C. J.; Wagoner, J.; Yu, Y.; van der Donk, W. A. Leader peptide establishes dehydration order, promotes efficiency, and ensures fidelity during lacticin 481 biosynthesis. *J. Am. Chem. Soc.* **2016**, *138*, 6436-44.
(33) Bobeica, S. C.; Zhu, L.; Acedo, J. Z.; Tang, W.; van der Donk, W. A. Structural determinants of macrocyclization in substrate-controlled lanthipeptide biosynthetic pathways. *Chem. Sci.* **2020**, *11*, 12854-70.
(34) Desormeaux, E. K.; Barksdale, G. J.; van der Donk, W. A. Kinetic analysis of cyclization by the substrate-tolerant lanthipeptide synthetase ProcM. *ACS Catal.* **2024**, *14*, 18310-21.
(35) Tang, W.; Thibodeaux, G. N.; van der Donk, W. A. The enterococcal cytolysin synthetase coevolves with substrate for stereoselective lanthionine synthesis. *ACS Chem. Biol.* **2016**, *11*, 2438-46.
(36) Brötz, H.; Bierbaum, G.; Leopold, K.; Reynolds, P. E.; Sahl, H. G. The lantibiotic mersacidin inhibits peptidoglycan synthesis by targeting lipid II. *Antimicrob. Agents Chemother.* **1998**, *42*, 154-60.
(37) Breukink, E.; Wiedemann, I.; van Kraaij, C.; Kuipers, O. P.; Sahl, H. G.; de Kruijff, B. Use of the cell wall precursor lipid II by a pore-forming peptide antibiotic. *Science* **1999**, *286*, 2361-4.
(38) Wiedemann, I.; Bottiger, T.; Bonelli, R. R.; Wiese, A.; Hagge, S. O.; Gutsmann, T.; Seydel, U.; Deegan, L.; Hill, C.; Ross, P.; Sahl, H. G. The mode of action of the lantibiotic lacticin 3147--a complex mechanism involving specific interaction of two peptides and the cell wall precursor lipid II. *Mol. Microbiol.* **2006**, *61*, 285-96.
(39) Oman, T. J.; van der Donk, W. A. Insights into the mode of action of the two-peptide lantibiotic haloduracin. *ACS Chem. Biol.* **2009**, *4*, 865-74.
(40) Oman, T. J.; Lupoli, T. J.; Wang, T.-S. A.; Kahne, D.; Walker, S.; van der Donk, W. A. Haloduracin α binds the peptidoglycan precursor lipid II with 2:1 stoichiometry. *J. Am. Chem. Soc.* **2011**, *133*, 17544-7.
(41) Islam, M. R.; Nishie, M.; Nagao, J.; Zendo, T.; Keller, S.; Nakayama, J.; Kohda, D.; Sahl, H. G.; Sonomoto, K. Ring A of nukacin ISK-1: a lipid II-binding motif for type-A(II) lantibiotic. *J. Am. Chem. Soc.* **2012**, *134*, 3687-90.
(42) Mascher, T.; Zimmer, S. L.; Smith, T. A.; Helmann, J. D. Antibiotic-inducible promoter regulated by the cell envelope stress-sensing two-component system LiaRS of *Bacillus subtilis*. *Antimicrob. Agents Chemother.* **2004**, *48*, 2888-96.
(43) te Winkel, J. D.; Gray, A. D.; Seistrup, K. H.; Hamoen, L. W.; Strahl, H. Analysis of antimicrobial-triggered membrane depolarization using voltage sensitive dyes. *Front. Cell Dev. Biol.* **2016**, *4*, 29.
(44) Benfield, A. H.; Henriques, S. T. Mode-of-action of antimicrobial peptides: membrane disruption vs. intracellular mechanisms. *Front. Med. Technol.* **2020**, *2*, 610997.
(45) Ashrafuzzaman, M.; Andersen, O. S.; McElhaney, R. N. The antimicrobial peptide gramicidin S permeabilizes phospholipid bilayer membranes without forming discrete ion channels. *Biochim. Biophys. Acta - Biomembr.* **2008**, *1778*, 2814-22.
(46) Hopfer, R. L.; Mehta, R.; Lopez-Berestein, G. Synergistic antifungal activity and reduced toxicity of liposomal amphotericin B combined with gramicidin S or NF. *Antimicrob. Agents Chemother.* **1987**, *31*, 1978-81.
(47) Salah Ud-Din, A. I. M.; Tikhomirova, A.; Roujeinikova, A. Structure and functional diversity of GCN5-related N-acetyltransferases (GNAT). *Int. J. Mol. Sci.* **2016**, *17*, 1018.

(48) Vetting, M. W.; LP, S. d. C.; Yu, M.; Hegde, S. S.; Magnet, S.; Roderick, S. L.; Blanchard, J. S. Structure and functions of the GNAT superfamily of acetyltransferases. *Arch. Biochem. Biophys.* **2005**, *433*, 212-26.
(49) Asamizu, S. Recent advances in discovery and biosynthesis of ribosomally synthesized and post-translationally modified peptides (RiPP)-derived lipopeptides. *Nat. Prod. Rep.* **2025**, *42*, 1622-38.
(50) Jangra, M.; Travin, D. Y.; Aleksandrova, E. V.; Kaur, M.; Darwish, L.; Koteva, K.; Klepacki, D.; Wang, W.; Tiffany, M.; Sokaribo, A.; Chen, X.; Deng, Z.; Tao, M.; Coombes, B. K.; Vázquez-Laslop, N.; Polikanov, Y. S.; Mankin, A. S.; Wright, G. D. A broad-spectrum lasso peptide antibiotic targeting the bacterial ribosome. *Nature* **2025**, *640*, 1022-30.
(51) Jumper, J.; Evans, R.; Pritzel, A.; Green, T.; Figurnov, M.; Ronneberger, O.; Tunyasuvunakool, K.; Bates, R.; Žídek, A.; Potapenko, A.; Bridgland, A.; Meyer, C.; Kohl, S. A. A.; Ballard, A. J.; Cowie, A.; Romera-Paredes, B.; Nikolov, S.; Jain, R.; Adler, J.; Back, T.; Petersen, S.; Reiman, D.; Clancy, E.; Zielinski, M.; Steinegger, M.; Pacholska, M.; Berghammer, T.; Bodenstein, S.; Silver, D.; Vinyals, O.; Senior, A. W.; Kavukcuoglu, K.; Kohli, P.; Hassabis, D. Highly accurate protein structure prediction with AlphaFold. *Nature* **2021**, *596*, 583-9.
(52) Iqbal, A.; Arunlanantham, H.; Brown Jr., T.; Chowdhury, R.; Clifton, I. J.; Kershaw, N. J.; Hewitson, K. S.; McDonough, M. A.; Schofield, C. J. Crystallographic and mass spectrometric analyses of a tandem GNAT protein from the clavulanic acid biosynthesis pathway. *Proteins* **2010**, *78*, 1398-407.
(53) Wolf, E.; Vassilev, A.; Makino, Y.; Sali, A.; Nakatani, Y.; Burley, S. K. Crystal structure of a GCN5-related N-acetyltransferase. *Cell* **1998**, *94*, 439-49.
(54) Berman, H. M., Westbrook, J., Feng, Z., Gilliland, G., Bhat, T. N., Weissig, H., Shindyalov, I. N., Bourne, P. E. The Protein Data Bank. *Nucleic Acids Res.* **2000**, *28*, 235-42.
(55) He, H.; Ding, Y.; Bartlam, M.; Sun, F.; Le, Y.; Qin, X.; Tang, H.; Zhang, R.; Joachimiak, A.; Liu, J.; Zhao, N.; Rao, Z. Crystal structure of tabtoxin resistance protein complexed with acetyl coenzyme a reveals the mechanism for β-lactam acetylation. *J. Mol. Biol.* **2003**, *325*, 1019-30.
(56) Neuwald, A. F.; Landsman, D. GCN5-related histone N-acetyltransferases belong to a diverse superfamily that includes the yeast SPT10 protein. *Trends Biochem. Sci.* **1997**, *22*, 154-5.
(57) Syriste, L.; Patel, D. T.; Stogios, P. J.; Skarina, T.; Patel, D.; Savchenko, A. An acetyltransferase effector conserved across *Legionella* species targets the eukaryotic eIF3 complex to modulate protein translation. *mBio* **2024**, *15*, e03221-23.
(58) Vetting, M. W.; Roderick, S. L.; Yu, M.; Blanchard, J. S. Crystal structure of mycothiol synthase (Rv0819) from Mycobacterium tuberculosis shows structural homology to the GNAT family of N-acetyltransferases. *Protein Sci.* **2003**, *12*, 1954-9.
(59) Bhatnagar, R. S.; Fütterer, K.; Farazi, T. A.; Korolev, S.; Murray, C. L.; Jackson-Machelski, E.; Gokel, G. W.; Gordon, J. I.; Waksman, G. Structure of N-myristoyltransferase with bound myristoylCoA and peptide substrate analogs. *Nat. Struct. Biol.* **1998**, *5*, 1091-7.
(60) Vicente-Garcia, C.; Colomer, I. Lipopeptides as tools in catalysis, supramolecular, materials and medicinal chemistry. *Nat. Rev. Chem.* **2023**, *7*, 710-31.
(61) Li, Y. Y.; Li, X. R.; Lu, J. L.; Cui, J. J.; Zhai, W.; Xiong, J.; Han, H.; Gao, K.; Lei, X.; Zhang, C. R.; Luo, S.; Dong, S. H. Discovery and biosynthesis of lipolasso

peptides reveal CoA-transferase for tyrosine lipidation of ribosomal peptides. *Org. Lett.* **2025**, *27*, 12148-53.
(62) Chen, J. Y.; Zhu, L.; Zhang, K. Y.; Berthold, D. A.; van der Donk, W. A. Co-opting the bacterial lipoprotein pathway for the biosynthesis of lipidated macrocyclic peptides. *bioRxiv* **2026**, doi: https://doi.org/10.1101/2025.10.31.685832.
(63) An, L.; Cogan, D. P.; Navo, C. D.; Jiménez-Osés, G.; Nair, S. K.; van der Donk, W. A. Substrate-assisted enzymatic formation of lysinoalanine in duramycin. *Nat. Chem. Biol.* **2018**, *14*, 928-33.
(64) Mukherjee, S.; van der Donk, W. A. Mechanistic studies on the substrate-tolerant lanthipeptide synthetase ProcM. *J. Am. Chem. Soc.* **2014**, *136*, 10450-9.
(65) do Amaral, S. C.; Xavier, L. P.; Vasconcelos, V.; Santos, A. V. Cyanobacteria: a promising source of antifungal metabolites. *Mar. Drugs* **2023**, *21*, 359.
(66) Ishibashi, M.; Moore, R. E.; Patterson, G. M. L.; Xu, C.; Clardy, J. Scytophycins, cytotoxic and antimycotic agents from the cyanophyte Scytonema pseudohofmanni. *J. Org. Chem.* **1986**, *51*, 5300-6.
(67) Todorova, A. K.; Juettner, F.; Linden, A.; Pluess, T.; von Philipsborn, W. Nostocyclamide: a new macrocyclic, thiazole-containing allelochemical from Nostoc sp. 31 (cyanobacteria). *J. Org. Chem.* **1995**, *60*, 7891-5.
(68) Crnkovic, C. M.; Krunic, A.; May, D. S.; Wilson, T. A.; Kao, D.; Burdette, J. E.; Fuchs, J. R.; Oberlies, N. H.; Orjala, J. Calothrixamides A and B from the cultured cyanobacterium Calothrix sp. UIC 10520. *J. Nat. Prod.* **2018**, *81*, 2083-90.
(69) Meeks, J. C.; Campbell, E. L.; Summers, M. L.; Wong, F. C. Cellular differentiation in the cyanobacterium *Nostoc punctiforme*. *Arch. Microbiol.* **2002**, *178*, 395-403.
(70) Yan, T.; Li, F.; Li, J.; Chen, F. Antifungal activity of ToAP2D peptide against *Sporothrix globosa*. *Front. Bioeng. Biotechnol.* **2021**, *9*, 761518.
(71) Rothstein, D. M.; Spacciapoli, P.; Tran, L. T.; Xu, T.; Roberts, F. D.; Serra, M. D.; Buxton, D. K.; Oppenheim, F. G.; Friden, P. Anticandida activity is retained in P-113, a 12-amino-acid fragment of histatin 5. *Antimicrob. Agents Chemother.* **2001**, *45*, 1367-73.